Inorg. Chem. **2002**, *41*, 5609–5614

Carboxylate-Bridged Copper(II)–Lanthanide(III) Complexes $[\{Cu_3Ln_2(oda)_6(H_2O)_6\}\cdot 12H_2O]_n$ (Ln = Dy, Ho, Er, Y; oda = Oxydiacetate)

Alberto C. Rizzi,[†] Rafael Calvo,*[,†] Ricardo Baggio,[‡] María Teresa Garland,[§] Octavio Peña,[||] and Mireille Perec*[,⊥]

Departamento de Física, Facultad de Bioquímica y Ciencias Biológicas, Universidad Nacional del Litoral and INTEC (CONICET-UNL), Güemes 3450, 3000 Santa Fe, Argentina, Departamento de Física, Comisión Nacional de Energía Atómica, Avda. del Libertador 8250, 1429 Buenos Aires, Argentina, Departamento de Física, Facultad de Ciencias Físicas y Matemáticas, Universidad de Chile, Avda. Blanco Encalada 2008, Casilla 487-3, Santiago, Chile, U.M.R. 6511, L.C.S.I.M. CNRS, Universite Rennes I, 35042 Rennes, France, and Departamento de Química Inorgánica, Analítica y Química Física, Facultad de Ciencias Exactas y Naturales, INQUIMAE, Universidad de Buenos Aires, Ciudad Universitaria, Pabellon II, 1428 Buenos Aires, Argentina

Received May 27, 2002

The hydrothermal reaction of Ln_2O_3 (Ln = Dy and Ho), $Cu(OAc)_2\cdot 2H_2O$, and oxydiacetic acid in the approximate mole ratio of 1:3:8 resulted in the formation of two new members of the isostructural series of polymers formulated as $[\{Cu_3Ln_2(oda)_6(H_2O)_6\}\cdot 12H_2O]_n$, crystallizing in the hexagonal crystal system, space group *P*6/*mcc* (No. 192). Temperature-dependent magnetic susceptibilities and EPR spectra are reported for the heterometallic compounds Cu–Dy **1**, Cu–Ho **2**, Cu–Er **3**, and Cu–Y **4**. The results are discussed in terms of the structure of the compounds, the electronic properties of the lanthanide ions, and the exchange interactions between the magnetic ions.

Introduction

Heterometallic copper(II)−lanthanide(III) compounds with the metal centers bridged by carboxylate groups are of relevance in solid-state technology[1−3] and as models for exchange interaction studies between spin carriers.[4−7] So far, reports on extended 3-D Cu(II)−Ln(III) compounds are rare as compared to those on discrete units. The high coordination number usually exhibited by the lanthanides should, however, favor the construction of extended solids, depending on the nature of the carboxylate bridging ligands. Among these, the oxydiacetate dianion (oda = $O_2CCH_2OCH_2CO_2$), having five potential oxygen-donor atoms, has been satisfactorily used by us and others in the assembling of lanthanide and copper ions in the 3-D series of complexes $[Cu_3Ln_2(oda)_6(H_2O)_6\cdot xH_2O]_n$, with Ln = Y,[8] Gd,[8,9] Eu,[8] Nd,[8,10] Pr,[8] Er,[10] and Yb.[11] All these crystallize in the hexagonal system, space group *P*6/*mcc*, and appear as appropriate models for investigating changes of exchange interactions between metal ions as the lanthanide element varies along the series. The homologous polymers for the two larger La and Ce ions have been recently found to crystallize in the hexagonal system, space group $P\bar{6}2c$.[12] Also relevant to the present study are the reported polymeric compounds involving $CuLn_2$ 1-D chains

* Authors to whom correspondence should be addressed. E-mail: rcalvo@dfbioq.unl.edu.ar (R.C.); perec@q1.fcen.uba.ar (M.P.). Fax: +54-342-457-5221 (R.C.); +54-11-4576-334 (M.P.).
† Universidad Nacional del Litoral and INTEC (CONICET-UNL).
‡ Comisión Nacional de Energía Atómica.
§ Universidad de Chile.
|| CNRS, Universite Rennes I.
⊥ Universidad de Buenos Aires.

(1) Segal, D. *Chemical Synthesis of Advanced Ceramic Material*; Cambridge University Press: Cambridge, U.K., 1989.
(2) Chanaud, P.; Julve, A.; Vaija, P.; Persin, M.; Cot, L. *J. Mater. Sci.* **1994**, *29*, 4224.
(3) Wang, S.; Pang, Z.; Smith K. D. L.; Wagner, M. J. *J. Chem. Soc., Dalton Trans.* **1994**, 955.
(4) Kahn, O.; Guillou, O. *New Frontiers in Magnetochemistry*; O'Connor, C. J., Ed., World Scientific: Singapore, 1993.
(5) Kahn, O. *Adv. Inorg. Chem.* **1995**, *43*, 179.
(6) Kahn, O. *Molecular Magnetism*; VCH: Weinheim, 1993.
(7) Kahn, M. L.; Mathoniere, C.; Kahn, O. *Inorg. Chem.* **1999**, *38*, 3692.
(8) Baggio, R.; Garland, M. T.; Moreno, Y.; Peña, O.; Perec, M.; Spodine, E. *J. Chem. Soc., Dalton Trans.* **2000**, 2061.
(9) Mao, J.-G.; Song, L.; Huang, X.-Y.; Huang, J.-S. *Polyhedron* **1997**, *16*, 963.
(10) Mao, J.-G.; Huang, J.-S.; Ma, J. F.; Ni, J.-Z. *Transition Met. Chem. (London)* **1997**, *22*, 277.
(11) Mao, J.-G.; Song, L.; Huang, J.-S. *Jiegou Huaxue* **1997**, *16*, 228.

10.1021/ic025754o CCC: $22.00
Published on Web 09/18/2002

(Ln = Sm, Gd, Pr, Nd) bridged by trichloroacetates,[13−15] the 1-D and 3-D Cu_3Gd_2 polymers bridged by 2,5-pyridinedicarboxylate, and the 3-D $CuGd_2$ and Cu_3Sm_2 polymers bridged by 2,4-pyridinedicarboxylate.[16]

We report herein the crystal structure and magnetic susceptibility measurements in two new compounds of the $[Cu_3Ln_2(oda)_6(H_2O)_6 \cdot xH_2O]_n$ series, those of Dy (Kramers ion) and Ho (non-Kramers ion). We also report susceptibility measurements in two other homologous compounds of the series, those of Y[8] ($4f^0$) and Er[10] (Kramers ion), compounds whose structures have been reported before. The magnetic data are used to investigate electronic properties of the magnetic ions, lanthanide and copper, and the interaction between them. According to the crystal structure, the exchange interactions between metal atoms (Cu···Cu, Cu···Ln, Ln···Ln) in this series of compounds are mediated through chemical bridges involving several atoms. Thus, the magnitudes of such interactions are expected to be small and difficult to evaluate from magnetic susceptibility measurements alone. For that reason, we also performed, and report here, EPR measurements in four nonmagnetic and magnetic Cu−Ln compounds. This technique allows us to obtain information about the magnitude of weak magnetic couplings, through spectral measurements performed at high temperatures. These magnetic interactions produce broadening and collapse of the resonances, and the EPR spectra give information about the magnitudes of the exchange and allow us to attribute them to specific superexchange paths.

Experimental Section

Materials and Methods. All of the starting materials, purchased from Aldrich, were used without further purification. C and H microanalyses were carried out with a Carlo Erba EA 1108 elemental analyzer. Copper was determined on a Shimadzu AA6501 spectrophotometer. Infrared spectra were recorded on a Nicolet FT-IR 510 P spectrophotometer using the KBr pellet technique. Thermogravimetric analyses were recorded on a Mettler TG-50 thermal analyzer under an atmosphere of air at a heating rate of 5 °C min^{-1}. Powder X-ray diffraction (XRD) data were collected using monochromated Cu Kα radiation on a Phillips X'Pert diffractometer. Temperature-dependent magnetic susceptibilities of solid samples were recorded on a SHE 906 SQUID susceptometer in the range 2−300 K. EPR measurements were performed in finely powdered samples at 9.778 GHz and 300 K, with a Bruker spectrometer using a rectangular cavity with 100 kHz field modulation.

Synthesis. $[\{Cu_3Dy_2(oda)_6(H_2O)_6\} \cdot 12H_2O]_n$ (1). Compound **1** was prepared from a mixture of Dy_2O_3 (0.25 g, 0.5 mmol), $Cu(OAc)_2 \cdot H_2O$ (0.3 g, 1.6 mmol), oxydiacetic acid (0.5 g, 3.8 mmol), and 50 mL of water in a stainless steel bomb at 120 °C for 48 h. After cooling slowly at room temperature, the compound was collected by filtration as a polycrystalline powder, washed with ethanol, and dried in air. Yield: 0.5 g, 60%. Found: C, 19.5; H, 4.2; Cu, 12.5. Calcd for $C_{24}H_{60}O_{48}Cu_3Dy_2$: C, 19.4; H, 4.1; Cu, 12.8%. Single crystals of **1** suitable for crystallographic work separated out from the filtered water solution after standing for three weeks. IR (KBr, cm^{-1}): 3430vs, br; 1599vs; 1478s; 1441vs; 1370m; 1318vs; 1248w; 1132s; 1063s; 1009w; 972m; 945m; 625s, br; 386m.

Table 1. Crystallographic Data for Compounds **1** and **2**[a]

	1	**2**
formula	$C_{24}H_{60}Cu_3Dy_2O_{48}$	$C_{24}H_{60}Cu_3Ho_2O_{48}$
fw, g/mol	1632.34	1637.20
a, *b* (Å)	14.424(1)	14.368(1)
c (Å)	15.187(1)	15.393(2)
V (Å^3)	2812.9(2)	2752.1(4)
ρ_{calcd}, g cm^{-3}	1.927	1.976
μ(Mo Kα), mm^{-1}	3.855	4.10
R1[b] [$F^2 > 2\sigma(F^2)$, all data]	0.039, 0.052	0.048, 0.076
wR2[c] [$F^2 > 2\sigma(F^2)$, all data]	0.106, 0.112	0.114, 0.129

[a] Features in common: $T = 23$ °C; system, hexagonal; $Z = 2$; space group, *P*6/*mcc* (No. 192); crystals, greenish-blue polyhedra; absorption correction, semiempirical. [b] $R1 = \sum||F_o| - |F_c||/\sum|F_o|$. [c] $wR2 = [\sum[w(F_o^2 - F_c^2)^2]/\sum[w(F_o^2)^2]]^{1/2}$.

$[\{Cu_3Ho_2(oda)_6(H_2O)_6\} \cdot 12H_2O]_n$ (2). The Ho complex (**2**) was synthesized by a similar procedure to that described for **1**, replacing Dy_2O_3 by Ho_2O_3. Yield: 0.6 g, 75%. Found: C, 17.8; H, 3.8; Cu, 11.8. Calcd for $C_{24}H_{60}O_{48}Cu_3Ho_2$: C, 17.7; H, 3.7; Cu, 11.5%. The IR spectrum was similar within ±5 cm^{-1} to that described in the preceding paragraph.

$[\{Cu_3Er_2(oda)_6(H_2O)_6\} \cdot 12H_2O]_n$ (3) and $[\{Cu_3Y_2(oda)_6(H_2O)_6\} \cdot 12H_2O]_n$ (4). These compounds were first prepared as reported in refs 10 and 8, respectively. Here, they were synthesized identically to compounds **1** and **2**, but with Er_2O_3 and Y_2O_3 used in place of Dy_2O_3 and Ho_2O_3, respectively. The yields were about 75% for the two compounds based on the amount of Ln_2O_3 used. Found for **3**: C, 17.8; H, 3.8; Cu, 11.5. Calcd for $C_{24}H_{60}O_{48}Cu_3Er_2$: C, 17.5; H, 3.7; Cu, 11.5%. Found for **4**: C, 19.5; H, 4.5; Cu, 12.5. Calcd for $C_{24}H_{60}O_{48}Cu_3Y_2$: C, 19.4; H, 4.1; Cu, 12.8%. The IR spectra are similar to those previously described, with absorption bands within ±5 cm^{-1}.

Crystallography. A summary of crystal parameters and data collection and refinement details is given in Table 1. Data were collected on a Bruker SMART 6000 diffractometer equipped with a CCD detector and graphite-monochromated Mo Kα ($\lambda = 0.71073$ Å) radiation. The unit cell parameters were determined by least-squares refinement of the whole, highly redundant data set ($2\theta \leq 50°$) collected by the ω scan technique and corrected for Lorentz and absorption effects. The starting model used for structure resolution was the one reported in ref 8. As found therein, the hydration water molecules appeared very elusive, and only a few of them, heavily disordered, could be located. A maximum number of 18 water molecules per formula unit was established by TGA in single-crystal samples. Refinement was performed by full-matrix least-squares in F^2, with anisotropic thermal parameters for the non-hydrogen atoms. Computer programs used in this study were SHELXL-97[17] and SHELXTL-PC[18] software packages.

(12) Liu, Q.-D.; Li, J.-R.; Gao, S.; Ma, B.-Q.; Liao, F.-H.; Zhou, Q.-Z.; Yu, K.-B. *Inorg. Chem. Commun.* **2001**, *4*, 301.

(13) Kutlu, I.; Meyer, G.; Oczko, G.; Legendziewicz, J. *Eur. J. Solid State Inorg. Chem.* **1997**, *34*, 231.

(14) Legendziewicz, J.; Borzechowska, M.; Oczko, G.; Meyer, G. *New J. Chem.* **2000**, *24*, 53.

(15) Voronkova, V. K.; Yablokov, Yu. V.; Legendziewicz, J.; Borzechowska, M. *Phys. Solid State* **1999**, *41*, 1976.

(16) (a) Liang, Y.; Cao, R.; Su, W.; Hong, M.; Zhang, W. *Angew. Chem., Int. Ed.* **2000**, *39*, 3304. (b) Liang, Y.; Hong, M.; Su, W.; Cao, R.; Zhang, W. *Inorg. Chem.* **2001**, *40*, 4574. (c) Liang, Y.; Cao, R.; Hong, M.; Sun, D.; Zhao, Y.; Weng, J.; Wang, R. *Inorg. Chem. Commun.* **2002**, *5*, 366.

(17) Sheldrick, G. M. *SHELXL-97: Program for the Refinement of Crystal Structures from Diffraction Data*; University of Gottingen: Gottingen, Germany, 1997.

(18) Sheldrick, G. M., *SHELXTL-PC. Version 4.2*; Siemens Analytical X-ray Instruments Inc.: Madison, WI, 1991.

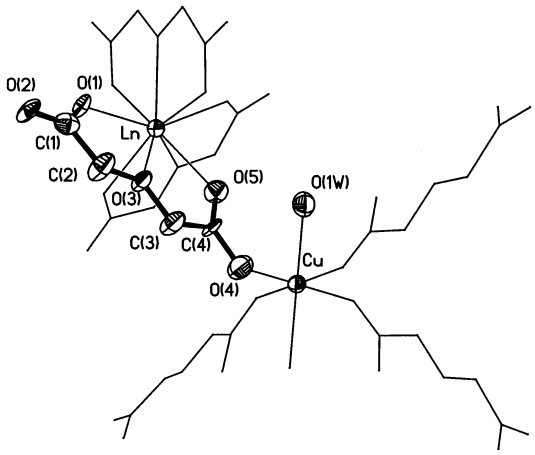

Figure 1. View of the Ln and Cu coordination polyhedra in the polymeric crystal structures showing the atom-labeling scheme at the 50% probability level.

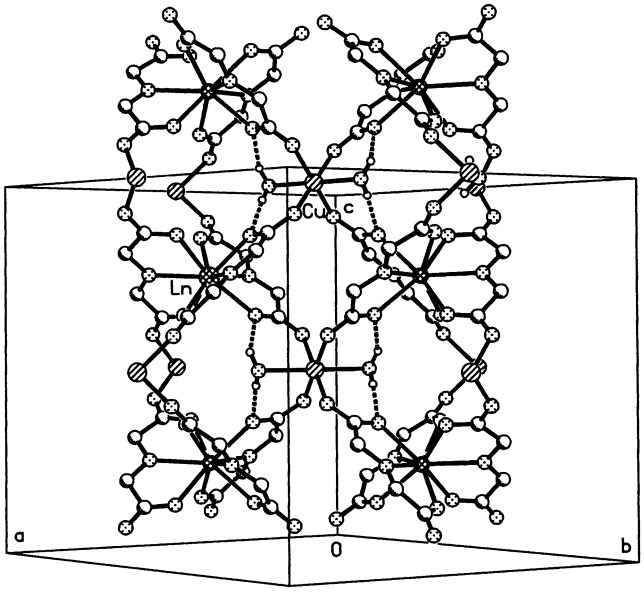

Figure 2. Packing view along the [110] direction. Hydrogen-bonding interactions involving aqua ligands only are shown.

Results

Synthesis. The hydrothermal reaction of Ln_2O_3, $Cu(OAc)_2 \cdot H_2O$, and oxydiacetic acid in the mole ratio 1:3:8 at 120 °C for 48 h led to the formation of blue single crystals of $[\{Cu_3Ln_2(oda)_6(H_2O)_6\}\cdot 12H_2O]_n$ complexes (where Ln = Dy, Ho, Er, Y) in high purity and yield. It is noteworthy that the present hydrothermal reactions afforded polymer networks analogous to those previously reported from the conventional self-assembly reactions with CuO.[9] The IR spectra, thermal stability, and powder X-ray diffraction patterns of the complexes are similar to those reported for the other members in the series.

Crystal Structures. The two polymers $[\{Cu_3Ln_2(oda)_6(H_2O)_6\}\cdot 12H_2O]_n$ (Ln = Dy **1**, Ho **2**) crystallize in the same hexagonal crystal system, space group *P*6/*mcc* (No. 192) and are built up from the two small and simple building blocks, LnO_9 and CuO_6, illustrated in Figure 1. These come together to build the 3-D framework of close-packed channels represented in Figure 2, which is also isostructural to those of the other members of the series for Ln = Y, Gd, Eu, Nd, Pr, Yb, and Er. Briefly, the Ln atom coordinates to two inner carboxylate oxygens and to the ether oxygen of three symmetry-related oda ligands to define a tricapped trigonal prismatic environment (TCTP).[19] In turn, each Cu atom coordinates to the remaining outer carboxylate oxygens of four oda anions and to two aqua ligands. Selected bond lengths and angles for the two compounds are summarized in Table 2. As expected, and because the ionic radius of Dy(III) (1.223 Å) is slightly larger than that of Ho(III) (1.212 Å), all of the metal−ligand bonds in the Cu−Dy compound are ca. 0.01 Å longer than the corresponding bonds in the Cu−Ho homologue; the bond angles in both compounds are very similar.

Table 2. Selected Bond Lengths (Å) and Angles (deg) for Compounds **1** and **2**[a]

	1	**2**
M−O(1)	2.381(3)	2.372(3)
M−O(3)	2.461(5)	2.450(5)
Cu−O(2)	1.948(3)	1.944(4)
Cu−O(1W)	2.495(5)	2.474(6)
O(1)−C(1)	1.258(5)	1.246(6)
O(2)−C(1)	1.242(5)	1.252(6)
O(3)−C(2)	1.391(5)	1.392(6)
C(1)−C(2)	1.502(6)	1.500(7)
O(1)−M−O(1)#1	127.1(2)	127.5(2)
O(1)#2−M−O(1)	85.7(2)	86.8(2)
O(1)#3−M−O(1)	79.56(12)	78.74(14)
O(1)−M−O(3)	63.56(8)	63.73(8)
O(1)−M−O(1)#4	146.5(2)	147.0(2)
O(1)−M−O(3)#5	137.16(8)	136.61(9)
O(1)−M−O(3)#3	73.26(8)	73.49(8)
O(3)−M−O(3)#5	120.	120.
O(2)−Cu−O(2)#6	180.0	180.0
O(1W)−Cu−O(1W)#6	180.0	180.0
O(2)−Cu−O(2)#7	91.7(2)	91.7(3)
O(2)−Cu−O(1W)	94.75(13)	94.8(2)
C(2)−O(3)−C(2)#1	114.2(6)	114.3(6)
O(2)−C(1)−O(1)	126.4(4)	126.1(3)
O(2)−C(1)−C(2)	115.9(4)	115.6(5)
O(1)−C(1)−C(2)	117.7(4)	118.2(4)
O(3)−C(2)−C(1)	109.1(4)	108.7(5)

[a] Symmetry transformations used to generate equivalent atoms: #1 $-y+1, x-y, z$; #2 $x, x-y, -z+1/2$; #3 $-x+y+1, -x+1, z$; #4 $-y+1, -x+1, -z+1/2$; #5 $-x+y+1, y, -z+1/2$; #6 $x, y, -z+1$; #7 $-x+2, -y+1, -z+1$.

Magnetic Data. The molar magnetic susceptibility $\chi(T)$ of compounds **1**−**4** was measured between 2 and 300 K, under an applied field of 50 mT (except for complex **4**, which was measured under a magnetic field of 100 mT). The experimental results for the temperature dependence of the product $T\chi(T)$ are shown as filled circles (●) in Figure 3a for the Cu−Y compound and in the insets of Figure 3b,c,d for the Cu−Dy, Cu−Ho, and Cu−Er compounds, respectively. Pascal's constants[6] were used to estimate the correction of the underlying diamagnetism of the yttrium-based compound **4**. Figure 3b−d also display the experimental values of $\chi^{-1}(T)$ for the Cu−Dy, Cu−Ho, and Cu−Er compounds (●). The empty circles (○) in Figure 3b−d were obtained by subtracting at each temperature the susceptibility measured for complex **4** to the observed susceptibility of these three complexes. In this way, the diamagnetic contribu-

(19) Albertsson, J. *Acta Chem. Scand*. **1968**, *22*, 1563.

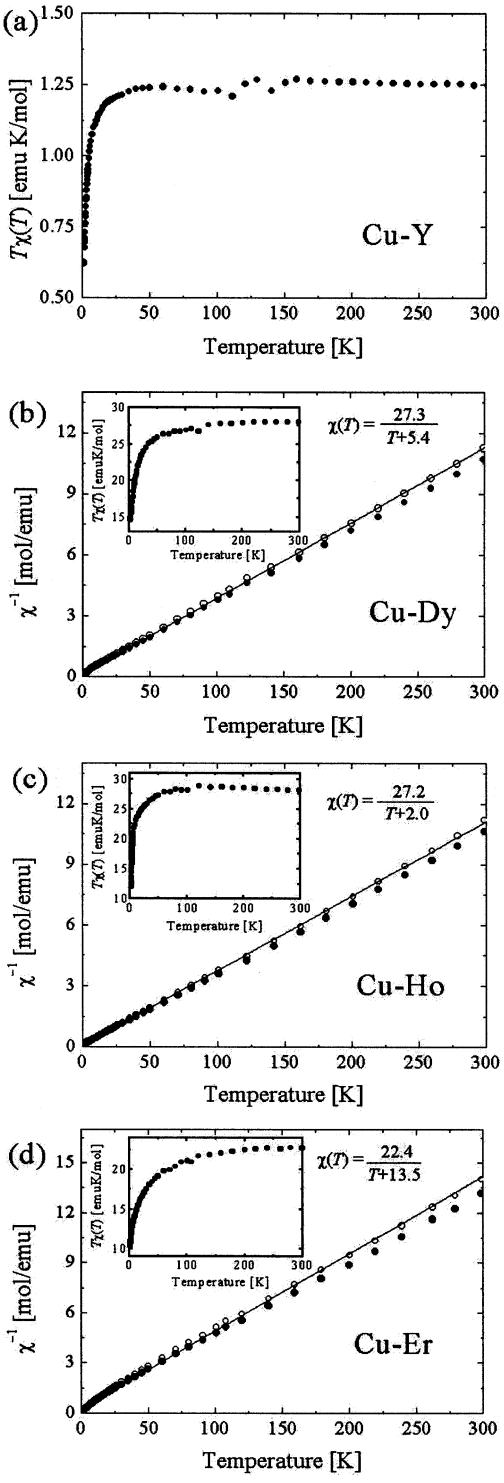

Figure 3. Results of the magnetic measurements [experimental data (●), data corrected as explained in the text (○)]: (a) plot of $T\chi(T)$ vs T for the Y−Cu compound **4**; (b, c, d) plots of values of the reciprocal $\chi^{-1}(T)$ vs T for the Dy−Cu **1**, Ho−Cu **2**, and Er−Cu **3** compounds. Curie plots of the corrected data are included. The insets display the values of $T\chi(T)$ for the corresponding compounds. The discontinuities in these plots in the 100−120 K range are due to instrumental problems.

tion and the magnetic contribution due to the copper "sublattice" were automatically subtracted from the total magnetism of the isostructural compounds, leaving just the contribution due to both the lanthanide ions and the coupling between the Ln(III) and the Cu(II) ions.

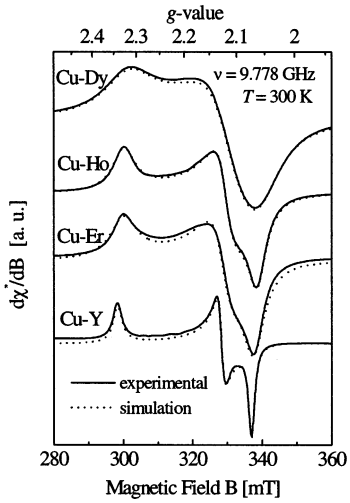

Figure 4. EPR spectra of the Cu−Dy, Cu−Ho, Cu−Er, and Cu−Y compounds. Solid lines (—) are the experimental spectra. Dotted lines (···) are obtained by simulations. The g-values and line widths obtained from the simulations are given in Table 4.

EPR Data. The EPR spectra observed at room temperature for the Cu−Ln polymers (Ln = Dy, Ho, Er, Y) are shown in Figure 4. In all cases, the observed spectrum is typical of $S = {}^1/_2$ copper spins and has a g-tensor having orthorhombic symmetry. No other EPR signals or hyperfine structure with the $I = {}^3/_2$ nuclear spin of the natural copper isotopes were observed.

Discussion

Magnetic Results. The results in Figure 3a for the product $T\chi$(T) for the yttrium-based copper complex **4** allow the determination of the underlying magnetism of the copper "sublattice". A practically constant value $T\chi(T) = 1.25$ emu K mol^{-1} is observed from room temperature down to 50 K. No contribution is expected from the nonmagnetic yttrium ions, and this high-temperature behavior corresponds to that expected for noninteracting $S = {}^1/_2$ spin. The calculated effective magnetic moment due to each of the Cu(II) ions, $\mu_{Cu} = 1.83\ \mu_B$, corresponds to a copper ion with an average g-factor $g = 2.12$, in agreement with the EPR results described later. At lower temperature, a pronounced decrease of the product $T\chi(T)$ is observed, reflecting a weak antiferromagnetic interaction between copper ions ($|J/k| < 1$ K).

The magnetic behavior is greatly modified when the nonmagnetic yttrium is replaced by the magnetic rare earths (Dy, Ho, and Er in Figure 3 b,c,d, respectively). The values of $\chi^{-1}(T)$ corrected as described previously were fitted by a Curie−Weiss law in a given range of temperature. Such range depends on the compound under study, being 20−300 K for compounds **1** (Cu−Dy) and **2** (Cu−Ho), and 50−300 K for compound **3** (Cu−Er). From the linear regression of the fit, we calculated the effective moment μ_{Ln}, per lanthanide ion, and the Curie temperature Θ. Table 3 gives these values of μ_{Ln} and Θ and, for comparison, includes the magnetic moment μ_{free} calculated for free Ln ions using[6]

$$\mu_{free} = g_J[J(J+1)]^{1/2}$$

Table 3. Magnetic Data for Complexes **1**, **2**, **3**, and **4**

cmpd	μ_{Cu}[a]	μ_{Ln}[b]	Θ (K)	$\mu_{free/Ln}$[c]
1 Cu−Dy	1.83	10.45	−5.4	10.65
2 Cu−Ho	1.83	10.45	−2.0	10.61
3 Cu-Er	1.83	9.50	−13.5	9.58
4 Cu−Y	1.83	0	−1.5	0

[a] Copper sublattice contribution per copper atom. The value observed for compound **4** was taken to be identical for the other three compounds. Throughout the table, magnetic moments are expressed in Bohr magnetons. [b] Lanthanide contribution per Ln ion, calculated from the data after subtraction of the copper sublattice contribution. [c] Value calculated for a free lanthanide ion, $\mu_{free} = g_J[J(J+1)]^{1/2}$.

The values of μ_{Ln}, obtained from the Curie plots, compare well with the moments theoretically expected for Ln(III) free ions. The small difference between experimental and theoretical moments may be attributed to a substoichiometry in lanthanide ion, estimated, at the most, to 3 or 4 at. % RE vacancies (RE = rare earth) per formula unit.

An important decrease of the product $T\chi(T)$ when lowering the temperature is seen below 80 K for complexes **1** and **2** in the insets of Figure 3b,c while a systematic decrease from almost room temperature is observed for the erbium-based compound **3** in the inset of Figure 3d. This behavior is certainly not due to the copper sublattice, because the decreases in the values of $T\chi(T)$ below 80 K in **1** and **2** and below room temperature in **3** are more pronounced than the decrease of the values for compound **4**. Also, it should be noted that the profile of the $T\chi(T)$ versus T curve for compound **4** is very similar to that reported for the Cu−Gd homologous compound.[8] Because the Gd(III) ion has an $^8S_{7/2}$ ground state, deviation from the Curie−Weiss law due to crystal field effects is minimal whereas deviation due to magnetic exchange interactions is expected to be comparable to that in compounds **1**−**3**. On this basis, the deviations from the Curie−Weiss law at high temperature for compounds **1**−**3** should be ascribed mainly to changes in the populations of the excited crystal-field levels. However, from the EPR results described later, we think that the decrease of $T\chi(T)$ versus T observed at low temperature should be mainly attributed to intramolecular antiferromagnetic-type exchange interactions between the Ln and Cu ions, separated across the carboxylate bridges by ca. 5.7 Å, having magnitudes of about 1 K.

EPR Results. The EPR spectra observed in the compounds with Dy and Er (magnetic rare earths, with Kramers degeneracy), with Ho (magnetic, but without Kramers degeneracy), and with Y (nonmagnetic) are very similar and characteristic of copper ions in an orthorhombic environment. Simulations of the spectra assuming anisotropic g-factors and line widths with angular variations having common axes were done for each case. The values of the parameters are given in Table 4, and the calculated spectra are displayed as dotted lines in Figure 4.

The span of the g-values of the spectra given in Table 4 is typical for Cu(II) ions with oxygen ligands. The difference of their values for compounds with different lanthanides is small and not very informative. The main difference in the spectra in Figure 4 is the intrinsic line width (see Table 4), which broadens and reduces the resolution of the spectra.

Table 4. Principal g-Factors and Line Widths ΔB (in mT) Obtained from Simulations of the EPR Spectra of Powder Samples Shown in Figure 4

	1 Cu−Dy	**2** Cu−Ho	**3** Cu−Er	**4** Cu−Y
g_1	2.064	2.069	2.069	2.073
g_2	2.120	2.120	2.127	2.128
g_3	2.316	2.328	2.329	2.342
ΔB_1	9.5	3.8	4.2	1.2
ΔB_2	9.4	4.1	4.9	1.5
ΔB_3	10.5	4.6	5.4	1.8

The line widths vary from an average value of 1.5 mT for the Y sample to 10.0 mT for the Dy sample. We did not expect to observe signals from Dy and Er in the corresponding compounds at room temperature, when their relaxation times are too short.

Considering that the copper ions in the studied compounds are in a nearly square geometrical arrangement, the rhombicity of the g-tensor observed with very similar values in compounds with magnetic and nonmagnetic rare earths is a surprising result. It appears in the Y compound, and thus, it is not produced by the magnetic interaction of the copper ions with the rare earths, but by interactions between the copper ions.

A rhombicity of the g-tensor may appear as a consequence of exchange interactions between copper ions, in a lattice where there are various chemically equal, but rotated, metal ion sites.[20] In the compounds studied here, there are six symmetry-related sites, and in principle, in a single-crystal EPR experiment, they would give rise to six spectra related one to another by rotations. The resonances corresponding to two of these sites, Cu_i and Cu_j having g-factors g_i and g_j, would collapse to a single resonance with a g-factor

$$g = (g_i + g_j)/2$$

average of the individual g-values, as a consequence of an exchange interaction J_{ij} between neighbor copper sites if

$$|J_{ij}| > |g_i - g_j|\mu_B B$$

where B is the magnetic field applied in the EPR experiment. In that case, the g-tensor corresponding to the collapsed resonance may have rhombic symmetry, even if the individual copper ions have axially symmetric g-tensors. This condition for the exchange interaction J_{ij} allows putting a lower limit on its magnitude when a collapse of the signals is observed. In our case, we estimate from the experimental result that

$$|J_{ij}|/k_B \geq 0.08 \text{ K}$$

between neighbor copper ions (at about 7.6 Å) in the studied compounds. According to the crystal structure of the Cu−Ln series, the superexchange paths connecting Cu ions are pairs of carboxylate bridges merging to a lanthanide ion, and involving seven atoms. The magnitude of the exchange interaction given previously is associated with these bridges.

(20) Calvo, R.; Mesa, M. A. *Phys. Rev. B* **1983**, *28*, 1244.

The broadening of the spectra for compounds with magnetic lanthanides, mainly for Ln = Dy, is associated with certainty to the exchange interactions between Cu and Ln (the results of the magnetic susceptibility measurements are ambiguous in this sense). It also involves the spin−lattice relaxation time T_1, which is very short at room temperature for the magnetic lanthanides, and should display important changes with temperature and with the rare earth involved. To undertake this problem, EPR measurements on single crystals at various temperatures are needed. The sizes required are considerably larger than those used herein for the X-ray studies. Thus, further work is now being directed toward the preparation of single crystals of sizes convenient for EPR measurements.

Conclusions

The following conclusions are drawn from this work: (i) The fast decrease of $T\chi(T)$ for the Y−Cu compound below 50 K (Figure 3a) indicates weak antiferromagnetic interaction between copper ions in the extended structures. (ii) The EPR spectrum of the Y−Cu sample allows us to set a lower limit $|J_{ij}|/k_B \geq 0.08$ K for these interactions between neighbor copper(II) ions. (iii) Comparative analyses of the profiles of the $T\chi(T)$ versus T curves for **1**−**4** indicate that at low temperatures antiferromagnetic Ln−Cu interactions are operative in these compounds. However, deviations from the Curie−Weiss law at higher temperatures in **1**−**3** indicate that changes with temperature of the populations of excited crystal-field effect levels may be important in these compounds. Susceptibility measurements alone are not conclusive in this point. (iv) The broadening of the EPR lines of the copper ions of powder samples of the compounds containing magnetic lanthanides (Dy, Ho, Er) can be unambiguosly attributed to Cu−Ln exchange interactions and to the short relaxation time of the magnetic lanthanide cations (Dy, Ho, and Er) in the lattice.

Acknowledgment. M.P. and R.C. are members of CONICET. This work was supported by CAI+D-UNL, Fundacion Antorchas and CONICET (Argentina) and PICS922 (Chile-France). The purchase of the Smart D-8 Discover diffractometer by Fundacion Andes C-13575 and Conicyt Fondap-11980002 (Chile) is gratefully acknowledged.

Supporting Information Available: Complete description of the X-ray crystallographic structural study. This material is available free of charge via the Internet at http://pubs.acs.org.

IC025754O